Dynamic Analysis and Control of a Roll Bending Process

Michael Hale and David E. Hardt

ABSTRACT: Recent research has shown that it is possible to automate the roll bending process using closed-loop control, which continuously calculates the springback of the metal workpiece. This means that one-pass forming of arbitrary two-dimensional workpiece shapes is now possible, subject to limitations of the physical apparatus and the controller. The identification of these limitations is the subject of this paper. Toward that end, dynamic models are developed for the individual components of the roll bending apparatus and for the process as a whole. These models include the unique nonlinearities of the roll bending system and also reflect the differences in the bending applications, such as bending and straightening. The process models are the basis for control analysis and design. An experimental roll bending apparatus is used to evaluate the system models and to verify the control design. The experimental results show that very good system response is possible using a simple controller. The results also illustrate the main limitation imposed on system response, which is due to vibration of the workpiece.

Introduction

The three-roll pyramid roll bender shown in Fig. 1 is a typical configuration for unidirectional bending, which consists of a pair of fixed outer rolls and a movable center roll. Bidirectional bending is possible if the single rolls are replaced by opposing roll pairs. One or more of the rolls are driven, and friction between the rolls and the workpiece permits the material to be rolled through the machine. As the workpiece moves, the position of the center roll is adjusted to produce a variable bend along the length of the workpiece. This process can be used to form large flat workpieces, e.g., metal plates used in boilers, or long thin workpieces, e.g., aluminum extrusions. In the aluminum industry, roll bending is used for straightening and contour correction of extrusions as well as for forming. This operation is normally controlled manually, and the accuracy of the final product shape is dependent on the skill of the operator.

The major obstacle preventing automation of roll bending has been material springback. In roll bending, the metal workpiece is plastically deformed as the workpiece moves through the machine. As the workpiece exits the bending apparatus, the elastic stresses in the metal are relaxed and the metal "springs back." Thus, the metal does not obtain its final shape until the workpiece has exited the machine. A method of calculating the springback while the workpiece is still loaded was presented by Hardt et al. [1]. Hale and Hardt [2] and Lee and Stelson [3] have extended the approach in [1] to include the roll-straightening process and have conducted experiments that show that with a closed-loop controller, straightening is nothing more than bending to zero curvature. The control scheme presented in [1] works well in the static or quasistatic case, but the productivity gains possible with this closed-loop curvature controller are limited by the assumption that workpiece feed rate will be very slow. This assumption was necessary to avoid unwanted oscillation and instability. In [1] and [2], the feed rates are kept below 0.7 in./sec. In [3], the workpiece was actually stepped through the bending device and the forming was performed while the workpiece was stationary. In order to increase the feed rate and exploit the inherent speed advantages of the roll bending process, it is necessary to redesign the controller. The system models necessary for control system design are presented along with an experimental evaluation of a proposed controller.

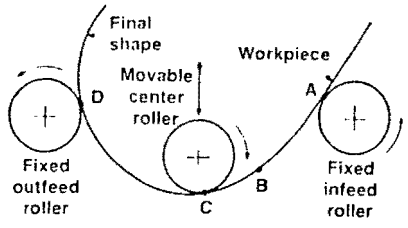

Fig. 1. Pyramid three-roll bender configuration.

Dynamic Analysis and Modeling

The closed-loop curvature control scheme for the roll bending process is based on real-time calculation of the material springback. As the workpiece is driven through the bending apparatus, the bending moment applied to the workpiece increases from zero at the input roll to a maximum at the center-roll contact point and then decreases to zero at the output roll. This loading sequence for a single point on the workpiece can be traced on the moment-curvature diagram (Fig. 2) and on the machine diagram (Fig. 1). At the input roll, the workpiece has zero moment and, assuming an initially flat workpiece, zero curvature (point A). The moment and curvature increase and the workpiece deforms elastically until the yield point is reached (point B). As the moment increases from point B to a maximum at point C, the workpiece deforms plastically. The moment and curvature decrease linearly as the workpiece moves from maximum loading (point C) to the output roll (point D), where the moment is again zero but the curvature is not because the workpiece has been plastically deformed. The slope of the unloading line in Fig. 2 is the same as the elastic loading line. From Fig. 2, the resulting unloaded curvature for each point on the workpiece is seen to be

$$K_u = K_L - M_{\max}/(dM/dK) \qquad (1)$$

where K_u is the unloaded curvature, K_l the loaded curvature, $M_{\max}$ the maximum applied moment, and dM/dK the slope of the elastic loading line. Equation (1) shows that it is possible to calculate the unloaded cur-

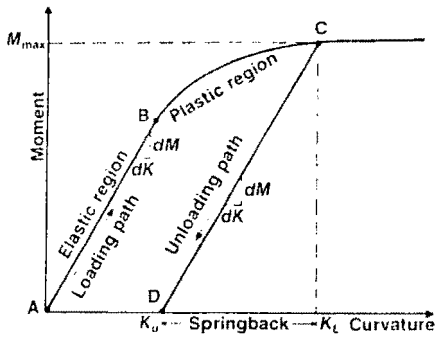

Fig. 2. Moment-curvature relationship.

Presented at the 1986 American Control Conference, Seattle, Washington, June 18-20, 1986. Michael Hale is a Research Assistant and David E. Hardt is an Associate Professor and Director for the Laboratory for Manufacturing and Productivity at the Massachusetts Institute of Technology, Cambridge, MA 02139.

0272-1708/87/0800-0003 $01.00 © 1987 IEEE

vature of the workpiece while the workpiece is in the loaded condition if the moment and curvature at the contact point under the center roll are known together with the elastic slope. This unloaded curvature measurement is used as feedback in the closed-loop control scheme for the roll bending system. A general block diagram of the control scheme is presented in Fig. 3. Changes in material properties, such as yield point, which can differ from workpiece to workpiece and even along the same workpiece, are reflected in the moment and curvature measurements and compensated for automatically. This was demonstrated for the quasistatic case in [1]-[3] using an integral controller. The integral controller was chosen to guarantee zero steady-state error. The feasibility of the closed-loop shape control scheme shown in Fig. 3 was demonstrated, but system response was very slow and bordered on instability. The models proposed subsequently provide the basis for a more complete controller design.

Although the system dynamics for any specific roll bending system will depend on the particular configuration and hardware under consideration, analysis of the bending process reveals five system components that are likely to contribute significantly to the system dynamics of any roll bending apparatus. These five components are the workpiece, the servo system, measurements and filters, disturbances, and the system controller. A model for each of these components is developed subsequently and verified with an experimental apparatus.

The experimental bending apparatus consists of two outer roll pairs and a center roll pair mounted on a Bridgeport milling machine. The outer roll pairs are fixed to the milling bed, which is driven by a servo-controlled DC motor through a ballscrew. The movement of the outer rolls with respect to the center roll provides the forming action needed. The center roll is mounted in and driven by the milling spindle. The workpiece is clamped between the pair of center rolls, and rotation of the spindle causes the workpiece to move through the apparatus. The loaded curvature is estimated using two linear variable differential transformers (LVDTs) mounted next to the center roll. The LVDTs measure the displacement of the workpiece, which can be used to calculate curvature. The displacement of the center roll can also be used to calculate loaded curvature [Eq. (3)] and is less noisy but also less accurate than the LVDT measurement. The maximum moment is calculated by multiplying the forces on the outer roll pair by the appropriate moment arms. The forces are measured with a strain-gage force transducer. A complete description of the experimental apparatus and details of the experimental procedure and measurement methods are given in [4].

Workpiece Model

As shown previously, it is not necessary to know anything about the plastic deformation of the workpiece as it is being loaded to calculate the unloaded curvature. It is necessary only to know the maximum moment and curvature at each point along the workpiece and the slope of the unloading path. For modeling purposes however, it is necessary to know how the workpiece deforms, both elastically and plastically, as a function of the center-roll position. For the workpiece model, we assume that the workpiece material is elastic perfectly plastic. If we further assume that the workpiece has a rectangular cross section that is constant along the length, then the relationship between moment and curvature for the entire loading path can be described, as shown in [5], by

$$M = K(dM/dK), \qquad K < K_y$$
$$M = 1.5M_y[1 - (K_y/K)^2/3], \qquad K \geq K_y \tag{2}$$

where M_y and K_y are the moment and curvature at yield. The assumption of a rectangular cross section is made to simplify the mathematics as well as the experimental apparatus but does not compromise the dynamic analysis.

The curvature of the point on the workpiece at the center-roll contact point can be expressed as a linear function of roll position using the deflection equation of a beam under three-point loading (see [6]),

$$K = 3z/L^2 \tag{3}$$

where z is the center-roll displacement and L is the distance between the center- and outer-roll axes. This relationship is based on linear beam theory but is a very good approximation well beyond yield, as seen in Fig. 4. Equation (3) is not dependent on material properties such as bending stiffness or yield point and is, therefore, very useful for a general model.

Substituting Eqs. (2) and (3) into Eq. (1) yields the following relationship between unloaded curvature and center-roll displacement (assuming an initially flat workpiece):

$$K_u = 0.0, \qquad z < z_y$$
$$K_u = \frac{3z}{L^2} - \frac{9z_y}{2L^2} + \frac{3}{2}\frac{z_y^3}{L^2 z^3}, \qquad z \geq z_y \tag{4}$$

where z_y is the center-roll position at the yield point of the workpiece. Equation (4) is the desired workpiece model, which relates the input (center-roll position) to the output (unloaded curvature). This equation applies to the point on the workpiece that is in contact with the center roll (point C in Fig. 2). This point corresponds to the maximum moment and curvature, which means that the final curvature of the workpiece is set at this point. Applying Eq. (4) to each point on the workpiece as it is rolled through the apparatus provides a model of the workpiece curvature as a function of the distance along the workpiece.

Figure 4 is a plot of measured moment scaled by the bending stiffness, loaded curvature, and unloaded curvature versus roll position for a $\frac{1}{4}$-in. × 1-in. 2024 aluminum strip, respectively. The loaded curvature was measured with the LVDTs. Equations (2)–(4) are also plotted using the bending stiffness and yield point obtained by experimentation. These plots show that the workpiece model developed previously is a reasonable approximation of the actual workpiece response.

There are three important features to note from the workpiece model. First, there is a deadband region while the workpiece is elastically loaded. The significance of the deadband region depends on the type of bending and the bending stiffness of the

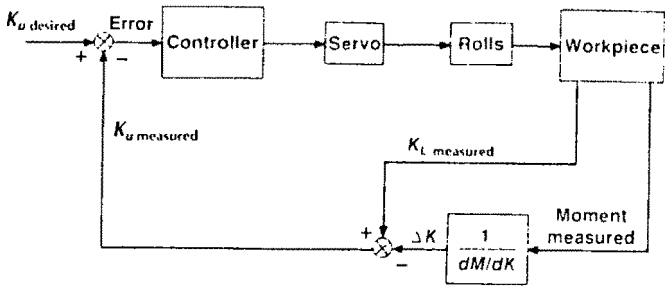

Fig. 3. Closed-loop control block diagram.

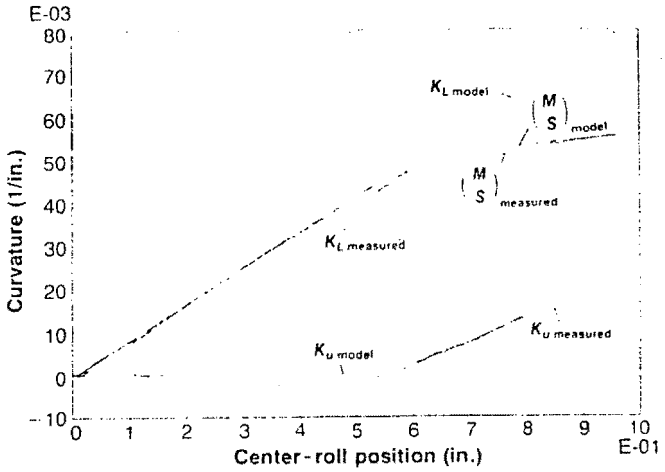

Fig. 4. Aluminum workpiece model, $\frac{1}{4}$ in. × 1 in.

workpiece. For very stiff workpieces, the elastic region and, therefore, the deadband region are very small. Flexible workpieces have a much larger deadband region. Forming circular shapes or bending workpieces with curvatures in only one direction involves passing through the deadband region only once; so the effect of the deadband will be small. For bidirectional bending or for straightening, the deadband region may dominate the operating region for a particular workpiece.

The second important feature of the workpiece model is the difference in response depending on whether the workpiece is stationary or moving through the rolls. For a stationary or very slow moving workpiece, hysteresis must be included in the model, as shown in Fig. 5. This is because the unloaded curvature does not change while the workpiece is in the elastic loading state or during unloading. If the workpiece is stationary, then only one point on the workpiece at the center-roll contact point is being formed. The center roll must load and unload the workpiece to give this point a final unloaded curvature. For a moving workpiece, each point is loaded as it moves from the infeed to the center roll and unloaded as it moves from the center to the outfeed roll. Therefore, the center roll does not have to move through a full forming sequence but merely moves to adjust the maximum forming depth. There is no hysteresis because each movement of the center roll acts on the new material being fed into the bending apparatus. The unloading occurs as the material moves from the center to the outfeed roll and does not depend on the center-roll movement. Figure 5 shows that a moving workpiece does not have hysteresis but still has a deadband region.

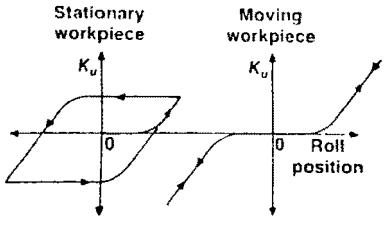

Fig. 5. Workpiece hysteresis.

The two cases shown in Fig. 5 are extremes. The stationary case assumes that a full forming cycle is performed on a single point of the workpiece. The moving case assumes that each movement of the center roll is applied to a point of the workpiece that is unaffected by all other points. Actual forming will fall between these two cases, but experiments show that the moving workpiece model is adequate if the rolling speed is such that the time required for a point on the workpiece to move from the center to the outfeed roll is greater than the rise time for the servo system.

The third important feature to note about the workpiece model is that time is not a variable in the model. The unloaded curvature is a function of center-roll position only. This means that the workpiece can be thought of as a nonlinear gain. This is, of course, an approximation because the workpiece does actually have mass, compliance, and damping, which all affect the system dynamics. In the workpiece model, these effects are assumed to be negligible. This assumption turns out to be a critical feature of the model, which is valid only under certain conditions.

Servo Model

Closed-loop control of the roll bender requires automatic control of the center roll by a servo system. At low frequencies, the servo system can be modeled as a standard position servo or velocity servo, depending on the particular application. The choice of a position or velocity servo becomes very important in the control analysis. The transfer function for a position servo is

$$\frac{z}{z_c} = \frac{\omega_n^2}{s^2 + 2\xi\omega_n + \omega_n^2} \tag{5}$$

where z_c is the position command, ω_n the natural frequency, and ξ the damping ratio. The transfer function for a velocity servo is

$$\frac{\dot{z}}{\dot{z}_c} = \frac{K}{\tau s + 1} \tag{6}$$

where $\dot{z}$ is the center-roll velocity, $\dot{z}_c$ the velocity command, K the servo gain constant, and τ the system time constant. Notice that this transfer function does not include the effect of the external load. For the experimental apparatus, the elastic load from bending is negligible because of the large reduction from the ballscrew.

The servo-control system on the experimental bending apparatus can be configured as either a velocity servo or a position servo. The velocity servo has a time constant of 0.042 sec. The servo gain constant K is adjustable but, for modeling purposes, is assumed to be 1.0 so that all of the system gains are lumped into the controller gain. The position servo used in the experiments is a critically damped second-order system with a bandwidth of 3.7 Hz.

Measurement and Filter Model

The transducers needed to measure maximum moment and loaded curvature will have a very large bandwidth compared to the servo system; so the dynamics of the measurements can be ignored. The signals must be filtered to eliminate high-frequency noise from the transducer signals and to reduce signal aliasing. The amount of filtering necessary and the break frequency of the filters will vary depending on the quality of the transducers, the required accuracy, the type of bending, and the sampling frequency. In any case, the filters can be modeled as a combination of first- and second-order differential equations. The filters used on all of the experimental transducers are second-order Butterworth filters with a break frequency of 130 Hz.

Disturbance Model

Initial curvature disturbances in the workpiece can be modeled as a shift of the moment-curvature curve, as shown in [2] and [4]. This shift is incorporated into the work-

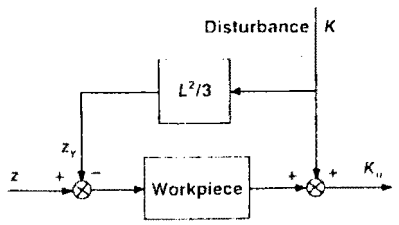

Fig. 6. Disturbance model block diagram.

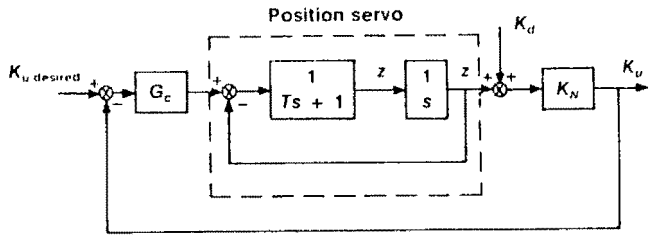

Fig. 7. Position-servo-based block diagram.

piece model by changing the yield point, as shown in Fig. 6. The disturbance curvature causes a change in the unloaded curvature that is equal to the disturbance curvature. This is shown as a direct addition in Fig. 6. The shift in the yield point is determined by applying Eq. (3). This is modeled as an additive term in Fig. 6, which affects the input to the workpiece model. Equation (7) is the model for the workpiece including curvature disturbance.

$$K_u = K_d, \qquad z < z_d + z_y$$

$$K_u = \frac{3(z - z_d)}{L^2} - \frac{9z_y}{2L^2} + \frac{3z_y^3}{2L^2(z - z_d)^2} + K_d, \qquad z \geq z_d + z_y \tag{7}$$

where K_d is the curvature disturbance and z_d is given by

$$z_d = K_d L^2/3 \tag{8}$$

Control

The models developed previously indicate that the roll bending system is very similar to a standard servo system. The servo is the major component of the system and contains most of the significant dynamics. However, the details of the servo/workpiece interaction introduce unique dynamic effects, which require more detailed analysis than the standard servo control problem. In particular, the deadband region and the presence of disturbances in the form of initial curvature are unique properties of the roll bending system. Also, the required bandwidth depends on both the spatial frequency of the desired input curvature and the rolling speed.

The feasibility of closed-loop control of the roll bending operation has been demonstrated using rudimentary control. The purpose of the control analysis and experiments described is to determine the ultimate limits of the roll bending system response and the practical factors unique to the roll bending process that limit the response. The control objective is to determine what control scheme or schemes can be used to attain this ultimate response. To compare the various control schemes, the following control criteria will be used to evaluate system response: stability, steady-state error, bandwidth, and disturbance rejection.

Control Analysis

The break frequency of the filters is very large compared with the break frequency of the position or velocity servo; so the filter dynamics are negligible compared with the servo dynamics. All of the following control analysis and design is done under the assumption of negligible filter dynamics.

The only nonlinearity in the component models derived previously is in the workpiece model. All other components are well represented by linear models. The full nonlinear model is used for simulation purposes; however, for analysis, much information can be gained by using a linearized model. Because the unloaded curvature is a nonlinear function of roll position only, the simplest linearized model is a constant gain operating on the roll position.

Using this model, consider the difference between a roll bending system based on a position servo and one based on a velocity servo when zero steady-state error is required for unloaded curvature. If the center roll is controlled by a position servo, then a change in servo position will result, through interaction with the workpiece, in a change in unloaded curvature if the system is past the deadband region. This correlates well with the workpiece model of a pure gain. If, however, the center roll is controlled by a velocity servo and the workpiece is a pure gain, then a step change in servo velocity should change the rate of change of unloaded curvature. This, in fact, does occur, but the controller is still sensing unloaded curvature and not rate of change of unloaded curvature. This means that an integration has occurred somewhere in the velocity servo interaction with the workpiece. In other words, because the unloaded curvature is a function of roll position only and not roll velocity, the workpiece operation on the servo velocity is actually a gain and an integration. Therefore, the workpiece model must be modified to include a free integrator as well as a gain for a roll bending system based on a velocity servo.

Figures 7 and 8 are block diagrams of the roll bending system based on a position servo and a velocity servo, respectively. The position servo block in Fig. 7 is drawn to emphasize the fact that the servo integrator is within the servo loop and is not a free integrator, which is necessary for zero steady-state error. The workpiece model in Fig. 7 is operating directly on position and does not contain an integrator. The workpiece model in Fig. 8 does contain a free integrator, which means that the system based on a velocity servo has the required zero steady-state error. A free integrator could be included in the controller of the position-servo-based system, but this would increase the order of the system, degrade system response, and decrease the relative stability of the system. The roll bending system based on a velocity servo for controlling the center roll appears to have many advantages over the position-servo-based system. It has good inherent steady-state error and stability properties. For these reasons, the roll bending system based on a position servo will be discarded at this

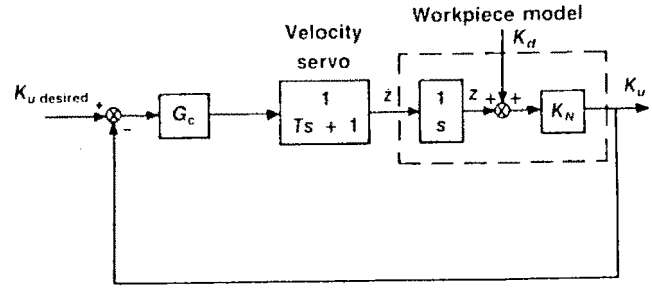

Fig. 8. Velocity-servo-based block diagram.

point and the control analysis will be continued for the velocity-servo-based system only.

If the velocity servo bandwidth is large enough, it might be possible to achieve an acceptable roll bending system bandwidth using a simple proportional controller at very low gains. Better system response could be attained by adding a zero to the system and drawing the poles to a position of higher bandwidth and greater stability, as shown in Fig. 9. Figure 9 was obtained from the s plane using pole-zero mapping. A zero can be added to the system either by including it in the controller or by feeding back the rate of change of output as well as the output. Measuring the rate of change of the output is the more attractive method because it is less affected by noise and also because the transient response has less overshoot for similar systems.

For the roll bending system, the output is unloaded curvature, which is calculated as detailed previously. The rate of change of unloaded curvature is much more difficult to measure. It is possible, however, to obtain a good approximation of the rate of change of unloaded curvature by using center-roll velocity. The relationship between roll position z and unloaded curvature K_u is given by Eq. (7). Taking the derivative of Eq. (7) gives

$$\dot{K}_u = \dot{K}_d, \qquad z < z_d + z_y$$

$$\dot{K}_u = \frac{3(\dot{z} - \dot{z}_d)}{L^2} - \frac{3z_y^3(\dot{z} - \dot{z}_d)}{L^2(z - z_d)^3} + \dot{K}_d, \qquad (9)$$

$$z \geq z_d + z_y$$

The rate of change of unloaded curvature depends on four variables: the roll position, z; roll velocity, $\dot{z}$; the curvature disturbance, K_d; and rate of change of curvature disturbance, $\dot{K}_d$. If the disturbances are small and all higher-order terms are negligible, then using only the following linear terms,

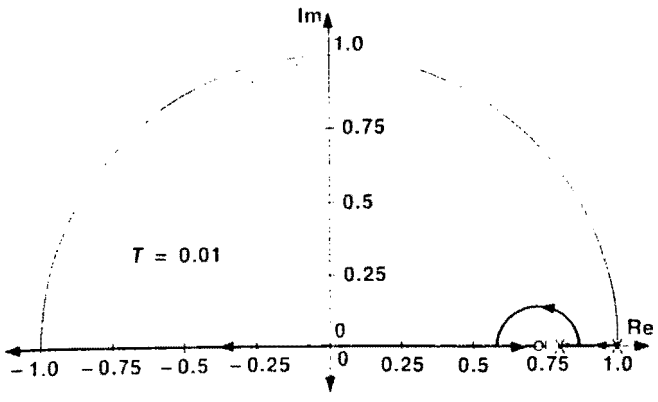

Fig. 9. z-plane root locus with a zero.

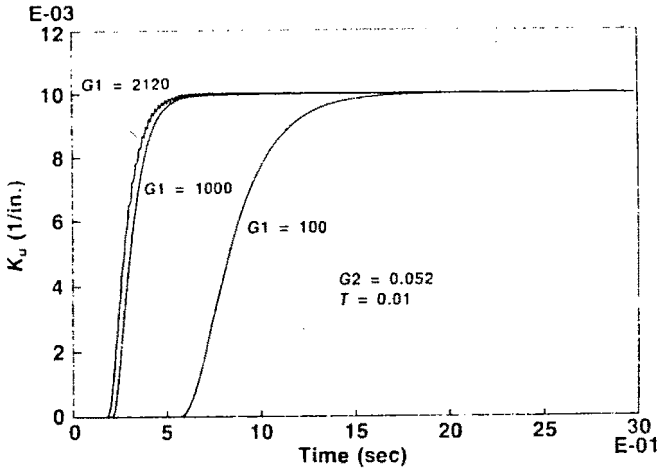

Fig. 10. Simulated system step response.

$$\dot{K}_u = 3\dot{z}/L^2 \qquad (10)$$

Notice that a controller using Eq. (10) as an estimate of $\dot{K}_u$ should provide slightly more damping and greater stability in the deadband region than if the true $\dot{K}_u$ were used. This is because, although $\dot{K}_u$ is zero in the deadband region (if $\dot{K}_d$ is zero), Eq. (10) indicates a rate of change in unloaded curvature proportional to the roll velocity.

If Eq. (10) is an accurate model of $\dot{K}_u$ and if the workpiece does actually perform an integrating function on the center-roll velocity, then a control scheme that uses a proportional controller and K_u plus $\dot{K}_u$ feedback should result in a roll bending system that has a root locus, as shown in Fig. 9. The control scheme as described is quite attractive because, with proper placement of the zero, the system will have very good stability robustness, zero steady-state error, high bandwidth, and good disturbance rejection. Also, a wide range of second-order system responses is possible by manipulation of the gain and the zero location.

The roll bending system described previously was simulated using a fourth-order Runge-Kutta integration technique to model the continuous system. The discrete controller used to implement the control action derived previously is

$$U = G1[K_{u\,\text{desired}} - K_u - (G2)(\dot{K}_u)] \qquad (11)$$

where U is the controller output, $G1$ is the controller gain, $G2$ is used to determine the location of the zero, and $\dot{K}_u$ is given by Eq. (10). The discrete controller time step is assumed to be $T = 0.01$ sec in the simulation.

The nonlinear workpiece model used in the simulation is given by Eq. (7). Notice that this equation models the loading deadband region but does not include any hysteresis. This means we only simulate a moving workpiece, but since we want to find the maximum feed rate, the moving-workpiece model is adequate. Equation (7) must be calibrated for a specific workpiece since the bending stiffness and the yield point are different for different materials and workpiece shapes. For the simulations and experiments shown subsequently, the workpiece modeled is a $\frac{1}{4}$-in. × 1-in. aluminum strip. The calibration factors used are taken from the experiment shown in Fig. 4. Figure 10 shows the results of the simulation at several different gains and with the zero located between the open-loop poles. For the simulations shown in Fig. 11, the zero location has been moved to the left of both poles, as shown in Fig. 9.

Experiments

There are several key assumptions in the control analysis that need to be examined experimentally. First, the assumption that the workpiece performs an integrating function

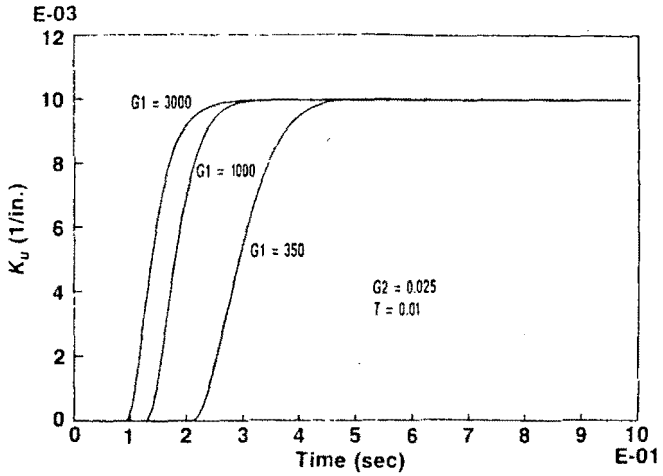

Fig. 11. Simulated system step response.

in conjunction with a velocity servo is crucial for zero error at steady state. The position of the integrator in the control loop is also important for the analysis of steady-state error to disturbances. Furthermore, the integrating workpiece assumption is the basis for choosing a velocity- rather than position-servo-based system. If the workpiece model is incorrect, then the control analysis is invalid. Second, the suggested control scheme uses a measurement of rate of change of unloaded curvature in the feedback signal. As mentioned earlier, $\dot{K}_u$ cannot be measured directly, but is assumed to be proportional to center-roll velocity. Since the $\dot{K}_u$ feedback is used to increase system damping and stability as well as to increase the system bandwidth, if the assumption is incorrect, there will be stability problems. The experimental objectives are to verify these assumptions and to determine the practical upper limits of the roll bending system response.

There are many practical factors that limit system performance. For the roll bending system, possible limitations are imposed by transducer bandwidth and noise, servo bandwidth and power, and controller design. However, because the objective is to explore the performance limits of the roll bending process, the experiments are designed to eliminate, as far as possible, limitations imposed by the hardware. The results provide some insight into the process limitations or the maximum system performance that can be attained given optimal conditions.

A short description of the experimental procedure is given subsequently. The details of the experimental method are given in [4]. The tests were performed using 2024-T6 aluminum workpieces with a rectangular cross section 1 in. wide and $\frac{1}{4}$ in. thick. The workpiece length varied from 3 to 6 ft. The experimental procedure for forming a workpiece follows:

- Load the workpiece in the bending apparatus and start the control program.
- Measure the bending stiffness of the workpiece.
- Turn on the center-roll drive motor to feed the workpiece through the bending apparatus.
- Begin real-time control of the unloaded curvature using the control algorithm developed previously.

Figures 12–15 show the response of the system to a step input of 0.01 in.$^{-1}$. For all tests shown, the workpiece feed rate is 13 in./sec and the loaded curvature is calculated from Eq. (3) using center-roll displacement. Figure 12 shows the results of the first experiment. The controller parameters listed on the plot are the same as for the simulation shown in Fig. 10. The results correspond very well with the simulation. The controller gain was increased for the second test, and the results, shown in Fig. 13, show a corresponding decrease in response time as expected. The small overshoot is due to error in the loaded curvature measurement. The system response is fast enough that a step command results in a small "kink" in the region close to the center roll. The center-roll position, unlike the LVDTs, does not accurately reflect rapid changes in curvature; so the curvature measurement is in error until the kink is past the forming region. A full discussion of the measurement error is given in [4].

Figures 12 and 13 verify the control analysis. In particular, the system has zero steady-state error and good stability even with the deadband nonlinearity. Although these tests demonstrate excellent system response, Fig. 11 suggests that even better sys-

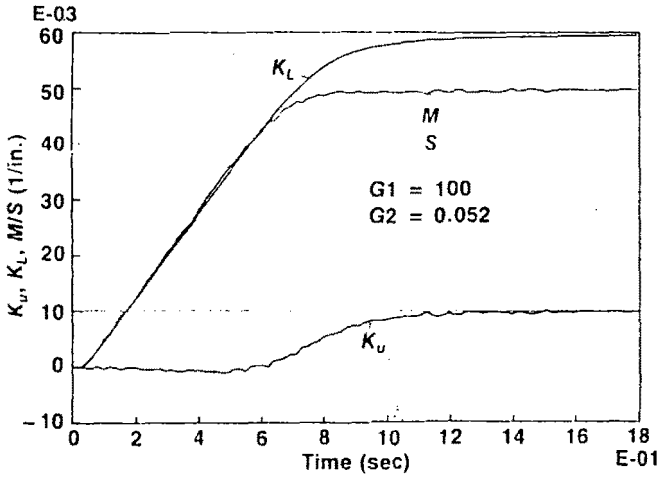

Fig. 12. Test 1.

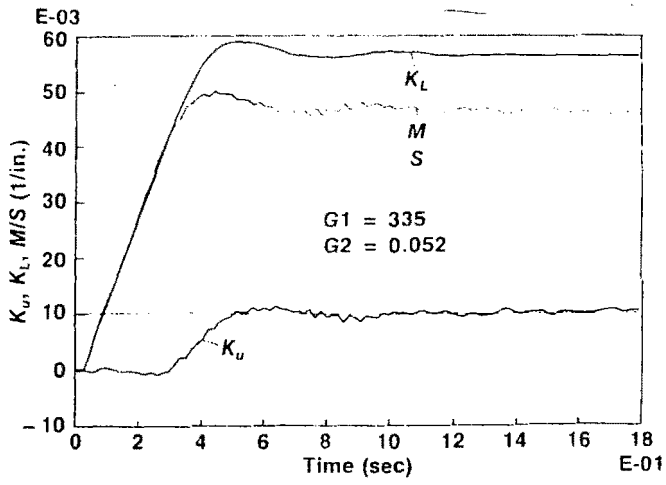

Fig. 13. Test 2.

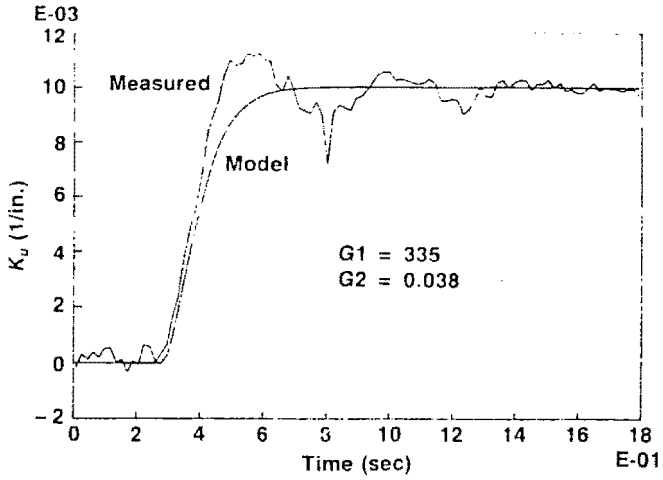

Fig. 14. Test 3.

tem response is possible if the zero location is moved to the location shown in Fig. 9. The results of the experiments conducted with the new zero position are shown in Figs. 14 and 15. The deadband and rise time have decreased in both tests, as expected from the simulation. Again there is some overshoot, which has been explained, but the error quickly settles to zero in Fig. 14. In Fig. 15, though, the system does not reach a steady state, but appears to be unstable. After the transient response, the unloaded curvature oscillates around the commanded curvature. Moreover, the oscillation appears to be at two different frequencies. A higher-frequency oscillation occurs between 0.6 and 1.0 sec, and a lower-frequency oscillation occurs from 1.2 to 1.8 sec. This oscillation is caused by the unmodeled dynamics of the workpiece. The vibration of the workpiece on the outfeed side of the bending apparatus causes "false readings" on the force transducer, which are interpreted through the moment measurement as fluctuations in the unloaded curvature. The actual workpiece shows no sign of the indicated curvature fluctuation, but, because it is indicated in the measurements, the controller responds to the apparent disturbances. This experiment shows that the workpiece dynamics, which are not considered in the system model, become significant as the system bandwidth is increased. A simple dynamic model of the workpiece can be used to explain the high- and low-frequency vibration shown in Fig. 15.

The dynamics of the portion of the workpiece on the outfeed side of the bending apparatus can be modeled very simply as the vibration of a cantilever beam. Because the workpiece is a continuous beam, there will be an infinite number of vibration modes and frequencies. However, the fundamental mode and natural frequency will be sufficient to explain the experimental results shown. The natural frequency of the fundamental mode for a cantilever beam, using the Euler beam model and assuming a uniform rectangular beam, is given by

$$\omega_n = 3.52\{EI/\rho L^4\}^{1/2} \qquad (12)$$

where ω_n is the natural frequency, EI the bending stiffness, ρ the material density, and L the length of the beam. Notice that the natural frequency is a function of beam length. This means that the natural frequency of the section of the workpiece on the outfeed side of the apparatus changes as the workpiece is fed through the machine. This explains why the oscillation frequency changes. At the beginning of the experiment, the overhanging workpiece is very short and has a natural frequency that is high compared to the system bandwidth. Therefore, the oscillation of the moment measurement caused by the workpiece vibration is sufficiently attenuated so that the vibration has very little effect on the system. As the workpiece moves through the apparatus, the natural frequency of the overhanging portion decreases and, at some point, the lower-frequency vibration becomes significant and interferes with the dynamics of the bending apparatus and controller.

The experiments shown in Figs. 12-15 show that the system responds to changes in the controller just as predicted by the control theory and simulation. This verifies that the roll bending system model contains all the significant dynamics, except for workpiece dynamics. As shown previously, the workpiece dynamics become important as the length of the overhanging workpiece increases and as the roll bending system bandwidth increases. The one unanswered question is how the closed-loop control system will respond to initial curvature disturbances.

Figure 16 shows the disturbance response of the roll bending system. The workpiece used for this disturbance test is the same workpiece that was formed in Fig. 14; so the workpiece has an initial curvature. After the forming test, the workpiece was reinserted into the bending apparatus and the disturbance experiment was run using a zero command for unloaded curvature. The controller parameters used were the same as in the forming test.

The test shows that the unloaded curvature initially decreases even though the system is moving to reject the disturbance, because the system still must move through the deadband region. In Fig. 16, the workpiece reaches the yield point at about 0.4 sec and the system settles to zero steady-state error in 1.0 sec. Notice that this response appears much

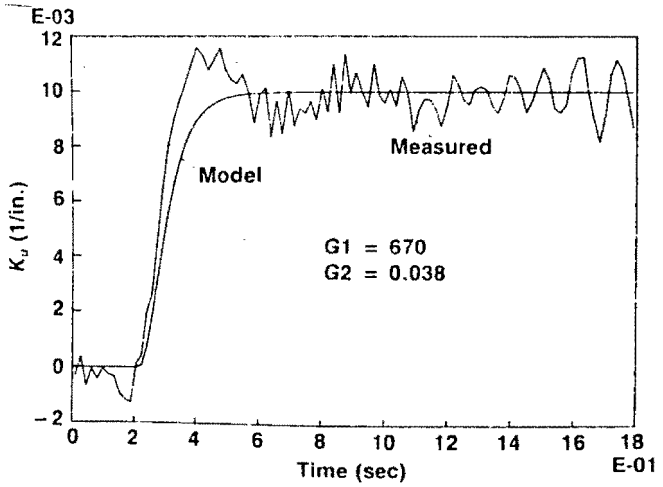

Fig. 15. Test 4.

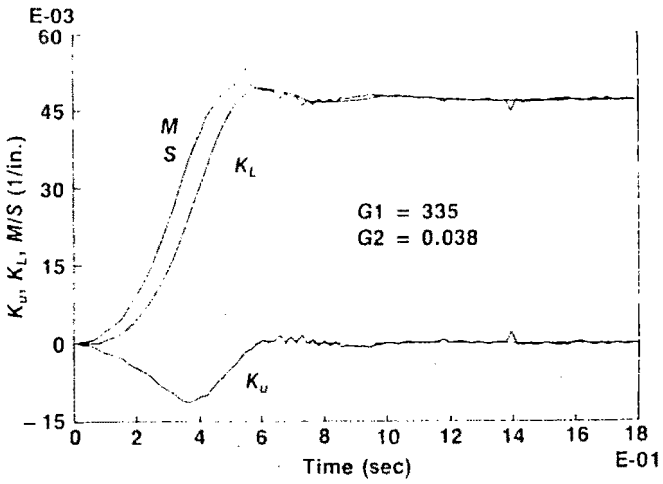

Fig. 16. Test 5.

cleaner than the response shown in Fig. 14. This is because the disturbance input is much smoother than the step command.

The disturbance test demonstrates excellent disturbance response characteristics with good transient response and zero steady-state error. This test also shows that the actual system response is much closer to the predicted response if the system is not hampered by the "kink effects" caused by the step command.

Conclusions

The experiments demonstrate that the roll bending system models are an accurate representation of the low-order dynamics of the roll bending process. The overall experimental system response corresponds very well with the simulated response, although there are small differences. This is to be expected however, because the simulation is based on fixed workpiece material properties while the actual workpiece properties vary. The material property variance is, in fact, a primary motivation for this research, because if the material properties are constant and well defined, an open-loop control system would work just as well and be much simpler to implement than the closed-loop controller presented in this research.

The primary assumptions used to develop the control scheme are that the workpiece performs an integrating function when the roll bending system is based on a velocity servo and that the center-roll velocity is a good approximation of the rate of change of unloaded curvature. The experiments show that the steady-state error in response to a step input goes to zero, which indicates a free integrator in the open-loop transfer function and verifies the workpiece model.

The use of center-roll velocity feedback to simulate $\dot{K}_u$ feedback was also very successful, as demonstrated by the experiments. The system responded to the velocity feedback in exactly the same manner as would be expected with true $\dot{K}_u$ feedback. This approximation is somewhat less successful at higher gains or as the system performance is pushed to the limit because the error inherent in the approximation becomes more significant, as do all errors at higher gains.

The experiments also show that the unmodeled higher-order dynamics, such as workpiece vibration, are significant except at relatively low gains. The vibration problem appears to be a rather severe process-related limitation on the maximum system response. As noted earlier, there are many hardware-related limitations, which can generally be overcome by the use of more powerful hardware. Higher-order dynamics are physical limitations of the particular process. In most control system designs, these higher-order effects can safely be ignored because they occur above a certain high frequency. The controller can be designed so that the system bandwidth is always safely below this critical frequency. The higher-order effects caused by workpiece vibration do not occur at a constant frequency, because the natural frequencies of the workpiece are a function of beam length. This means that the dynamic behavior of the workpiece changes during the bending operation. To safely ignore the vibration effects, the system bandwidth must be kept well below the lowest natural frequency of the overhanging workpiece. Therefore, the controller must be designed for the worst case. This imposes severe restrictions on maximum system performance, which cannot be removed by the use of better hardware.

References

[1] D. E. Hardt, M. A. Roberts, and K. A. Stelson, "Closed-Loop Shape Control of a Roll Bending Process," *Trans. ASME, J. Dyn. Systems, Measurement and Control*, vol. 104, pp. 317-322, Dec. 1982.

[2] M. B. Hale and D. E. Hardt, "Closed Loop Control of a Roll Straightening Process," *An CIRP*, vol. 33, pp. 137-140, Aug. 1984.

[3] M. Lee and K. A. Stelson, "Adaptive Control for a Straightening Process," *Sensors and Controls for Automated Manufacturing and Robotics*, ASME, New York, pp. 153-166, 1984.

[4] M. B. Hale, "Dynamic Analysis and Control of a Roll Bending Process," M.S. thesis, Massachusetts Institute of Technology, Cambridge, MA, 1985.

[5] S. H. Crandall, N. C. Dahl, and T. J. Lardner, editors, *An Introduction to the Mechanics of Solids*, Second edition, New York: McGraw Hill, pp. 455-477, 1959.

[6] N. H. Cook, *Mechanics and Materials for Design*, New York: McGraw Hill, pp. 255-260, 1984.

Michael Hale received the B.S. degree in 1983 from Oklahoma State University and the S.M. degree in 1985 from the Massachusetts Institute of Technology, both in mechanical engineering. He is currently a Ph.D. candidate and research associate at the Massachusetts Institute of Technology. His interests are in control of manufacturing processes, with particular interest in metal-forming, welding, and fabrication processes.

David E. Hardt is an Associate Professor of Mechanical Engineering and Director (since September 1985) of the Laboratory for Manufacturing and Productivity. This lab is an interdisciplinary focus for research and education in manufacturing processes and systems primarily related to the mechanical industries. Professor Hardt received the B.S. degree from Lafayette College in 1972, and the S.M. and Ph.D. degrees from the Massachusetts Institute of Technology (MIT) in 1974 and 1978, respectively, all in mechanical engineering. Since joining the MIT

faculty in 1979, he has pursued research in modeling, measurement, and control of manufacturing processes. This work has concentrated primarily on sheet metal forming and fusion welding processes, and has lead to novel concepts for greatly improving the performance of these operations. His research interests also include control of composite material processing and the manufacturing/design integration problem.

The sheet forming work has established the basis for in-process sensing and control of the deformation process and has been extended from two- to three-dimensional forming work. It has also encompassed real-time control of sheet formability as well as part geometry control. The welding research has concentrated on new methods for sensing and control of both the geometric and thermal properties of a weld. Based on a true closed-loop control philosophy, the physically coupled nonlinear, stochastic nature of welding is being treated in a comprehensive manner. This work has led to sensing techniques for weld penetration, adaptive control methods for increased dynamic performance, and decoupling control of a multivariable welding process. These research programs are sponsored by industry and government and currently involve the efforts of over 10 graduate assistants. Beginning in 1979, this research has involved over 30 M.S. theses and 7 Ph.D. students, as well as the efforts of several dozen undergraduates. The work has also been documented in over 30 technical papers and two chapters of a forthcoming book on basic manufacturing.

Professor Hardt is active with the ASME Dynamic Systems Division and serves as the Chairman of the Technical Panel on Manufacturing. This panel has organized several symposia targeted to the area of manufacturing process modeling and control. He has also served as consultant to the National Materials Advisory Board of the National Research Council. He has taught subjects in engineering mechanics, mechanical behavior of materials, instrumentation, dynamics, and classical control principles. In addition, he has developed a new graduate-level subject in the area of control of manufacturing processes, and is preparing a new text based on this subject. He has consulted on topics related to his research as well as mechanical engineering in general and has presented over 20 invited seminars to industry, universities, and technical societies on the topics of closed-loop manufacturing process control, flexible manufacturing systems, and robotics.

1987 CDC

The IEEE Conference on Decision and Control (CDC) will be held December 9–11, 1987, at the Westin Century Plaza Hotel in Los Angeles, California. The General Chairman of the conference is Professor William S. Levine of the University of Maryland. The Program Chairman is Professor John Baillieul of Boston University. The conference will include both contributed and invited sessions in all aspects of the theory and application of systems involving decision, control, optimization, and adaptation.

The plenary speeches will feature two talks on the Philosophy of Control and Systems Engineering. On Wednesday, December 9, Professor Stephen C. Jacobsen of the University of Utah Center for Biomedical Design will speak on the design and control of very complex mechanical systems. He will highlight his talk with personal thoughts and historical observations on the control of devices such as the 16-degree-of-freedom Utah/MIT dextrous robotic hand, which was designed and built under his direction at the center.

On Friday, December 11, Professor Jan C. Willems of the Mathematics Institute, University of Groningen, will speak about "Paradigms and Puzzles in Modeling Dynamical Systems." This will be a talk dealing with the speaker's ideas on the mathematical and philosophical foundations of system identification or modeling on the basis of observations.

We urge you to attend this premier control conference held in the dynamic and historic setting of Los Angeles. The pictures here illustrate a few of the many attractions of the Los Angeles area. For further information, contact the General Chairman:

Prof. William Levine
Dept. of Electrical Engrg.
University of Maryland
College Park, MD 20742
Phone: (301) 454-6841

Olvera Street, the oldest street in Los Angeles, has an authentic Old Mexico flavor and is a "must" see on a visit to Los Angeles.

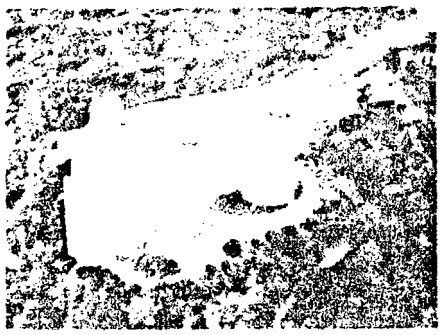

Griffith Park Observatory—"On a clear day you can see forever," and even further with the aid of the high-powered telescope at the park.

The La Brea Tar Pits have models and exhibits of saber tooth tigers, mastadons, and dire wolves.